REPORT DOCUMENTATION PAGE

AFOSR-TR-97

0278

1. AGENCY USE ONLY (Leave blank)	2. REPORT DATE	3. REPORT TYPE AND DATES COVERED
	1-7-1997	Final Tech 4-1-95 to 5-15-96

4. TITLE AND SUBTITLE

(U)Development of Predictive Reaction Models of Soot Formation (Soot Formation)

5. FUNDING NUMBERS

PE - 61102F
PR - 2308
SA - BS
G - F49620-94-1-0226

6. AUTHOR(S)

Dr. Brian Weiner

7. PERFORMING ORGANIZATION NAME(S) AND ADDRESS(ES)

Pennsylvania State University
110 Technology Center Bldg.
University Park, PA 16802-7000

8. PERFORMING ORGANIZATION REPORT NUMBER

Final Technical

9. SPONSORING / MONITORING AGENCY NAME(S) AND ADDRESS(ES)

AFOSR/NA
110 Duncan Avenue, Room B115
Bolling AFB, DC 20332-8080

10. SPONSORING / MONITORING AGENCY REPORT NUMBER

11. SUPPLEMENTARY NOTES

12a. DISTRIBUTION / AVAILABILITY STATEMENT

Approved for public release. Distribution is unlimited.

12b. DISTRIBUTION CODE

ABSTRACT (Maximum 200 words)

This report summarizes the work performed at the Pennsylvania State University during the period 04/01/95-05/15/96. Two studies are included in this report, one carried out by Kazakov and Frenklach and the other by Weiner and Frenklach. The first one examined the relative importance of acetylene versus PAH's as major species influencing soot mass growth rates according to the kinetic model developed by Frenklach et al. The other is a preliminary investigation of the initial steps of a reaction pathway by which C_4H_5 radicals can be converted by acetylene to PAH's. In the first study two proposed mechanisms for the initial stages of soot formation were compared. One mechanism postulates that PAH deposition on the soot surface plays the major role in soot mass growth, the other that growth is dominated by the contribution of C_2H_2, while the PAH condensation on soot surface is negligible. A kinetic analysis was applied to experimental results and showed that they are consistent with the predictions of the acetylenic mechanism. In the second study a reaction pathway starting from C_4H_5 radicals and leading to an aromatic radical in an acetylenic atmosphere was studied. This pathway was shown to be feasible on energetic grounds and involves a novel rearrangement from a five membered ring to a six membered aromatic ring via a tricyclic intermediate.

14. SUBJECT TERMS	15. NUMBER OF PAGES
soot, poly aromatic hydrocarbon, combustion	23
	16. PRICE CODE

17. SECURITY CLASSIFICATION OF REPORT	18. SECURITY CLASSIFICATION OF THIS PAGE	19. SECURITY CLASSIFICATION OF ABSTRACT	20. LIMITATION OF ABSTRACT
Unclassified	Unclassified	Unclassified	UL

Contract Grant F49620-94-1-0226

Final Report

to

Air Force Office of Scientific Research

Bolling AFB, DC 20332-8080

SOOT FORMATION

Brian Weiner

Department of Physics

Pennsylvannia State University

University Park, PA 16802

Table of Contents

This report summarizes the work performed at the Pennsylvania State University during the period 01/04/95 - 15/05/96. The Principal Investigator for part of this period, 08/01/95 - 15/05/96 was Dr. Brian L Weiner, while the Principal Investigator for the other part of this period, 01/04/95 - 08/01/95 was Dr. Michael Frenklach, the graduate student Andrei Kazakov was coinvestigator during all of this period. Two studies are included in this report, one carried out by Kazakov and Frenklach and the other by Weiner and Frenklach. The first one examined the relative importance of acetylene versus PAH's as major species influencing soot mass growth rates according to the kinetic model developed by Frenklach et al. The other is a preliminary investigation of the initial steps of a reaction pathway by which C_3H_3 radicals can be converted by acetylene to PAH's.

SUMMARY OF ACCOMPLISHMENTS;

Theses;

A. Kazakov "A computational study of the effect of pressure on soot formation in laminar premixed flames." July 1996.

Presentations;

A. Kazakov and M. Frenklach, 'Modeling of Soot Coagulation and Aggregation at High-Pressure Conditions', Fall Technical Meeting of the Eastern States Section of the Combustion Institute, Worcester, MA, 1995, pp. 415-418.

A. Kazakov and M. Frenklach, 'Dynamic Modeling of Soot Particle Coagulation and Aggregation in High-Pressure Laminar Premixed Flames', Work-in-Progress Poster Paper 140, presented at 26th Symposium (International) on Combustion, Naples, Italy, July 30, 1996.

SUMMARY OF RESEARCH:

On Roles Of PAH And Acetylene As Soot Growth Species;

A. Kazakov and M. Frenklach

The predictions of the present model indicate that, for both 1 and 10-bar C_2H_4-air premixed flames, soot mass growth rates are dominated by the contribution of C_2H_2, while the PAH condensation on soot surface is negligible. On the other hand, Howard and co-workers argued in their recent studies (Marr et al. 1994, Benish et al. 1995) that soot growth proceeds mainly through PAH deposition on the soot surface. Since the most recent work (Benish et al. 1995) has been carried out for atmospheric ethylene-air flames, it is of interest to compare the present model predictions with the analysis of the experimental results conducted by Benish et al.

Benish et al. studied two C_2H_4-air laminar premixed flames with the equivalence ratios equal 2.1 and 2.4. Tar material (PAH) and soot were collected at the different locations above the burner and weighted. The results were reported in mass units (mg/L) as a functions of distance from the burner. The analysis of the relative contributions of PAH and C_2H_2 to soot mass growth was conducted using the following equations:

$$\frac{dM_{soot}}{dt} = \gamma_{C_2H_2-soot} Z_{C_2H_2-soot} m_{C_2H_2} + \gamma_{tar-soot} Z_{tar-soot} m_{tar}, \quad (1.1)$$

$$\frac{dM_{tar}}{dt} = \gamma_{C_2H_2-tar} Z_{C_2H_2-tar} m_{C_2H_2} - \gamma_{tar-soot} Z_{tar-soot} m_{tar}, \quad (1.2)$$

where M_{soot} and M_{tar} are the masses of soot and tar, respectively, © collision efficiency, Z collision rate calculated from kinetic theory, m_{C2H2} and m_{tar} molecular weights of acetylene and tar, respectively.

The assumptions used to analyze the data are summarized below:

1) the average PAH collision diameter is estimated to be 10 Å, and the average PAH molecular weight is 500 g/mol;
2) soot mass density is 1.8 g/cm^3, all particles are of the same size; the particle number density is equal 10^{11} cm^{-3} and independent of the height from the burner;
3) the temperature is equal to 1650 K and independent of the height from the burner;;
4) the acetylene mole fraction is equal to 0.02 and independent of the height from the burner;
5) collision efficiencies of C_2H_2-soot and C_2H_2-tar are equal.

Upon application of these assumptions, Eqs. (1.1) and (1.2) can be rewritten as (see Appendix)

$$\frac{dM_{soot}}{dt} = 1.69\times 10^3 M_{soot}^{2/3}\gamma_{C_2H_2-soot} + 1.0\times 10^8 M_{tar}M_{soot}^{2/3}\gamma_{tar-soot}, \quad (1.3)$$

$$\frac{dM_{tar}}{dt} = 7.8\times 10^6 M_{tar}\gamma_{C_2H_2-tar} - 1.0\times 10^8 M_{tar}M_{soot}^{2/3}\gamma_{tar-soot}. \quad (1.4)$$

In Eqs. (1.3) and (1.4), M_{soot} and M_{tar} are given in units g/cm^3, time is in seconds. The rates of soot and tar mass growth were evaluated by the differentiation of the experimental curves.

The solution of the system (1.3) – (1.4) is obvious. Performing the summation of equations and using the assumption (5), one can obtain

$$\gamma_{C_2H_2-tar} = \gamma_{C_2H_2-soot} = \frac{dM_{soot}/dt + dM_{tar}/dt}{7.8\times 10^6 M_{tar} + 1.69\times 10^3 M_{soot}^{2/3}}, \quad (1.5)$$

and

$$\gamma_{tar-soot} = \frac{1.0\times 10^{-8}}{M_{tar}M_{soot}^{2/3}}\left(\frac{dM_{soot}}{dt} - 1.69\times 10^3 M_{soot}^{2/3}\gamma_{C_2H_2-soot}\right). \quad (1.6)$$

Using the described analysis, Benish et al. concluded that tar contributes from 80 to 94 % of soot mass increment for the flames studied.

While the simulations of the flames considered by Benish et al. were not carried out due to the lack of the input data, the modeling results for a similar, 1-bar ethylene-air flame studied experimentally by Jander, Wagner and co-workers (Jander 1992) are available (Kazakov et al. 1995). This flame has the same stoichiometry, $f = 2.1$ and, therefore, can be used for qualitative analysis of the observed trends.

According to the original experimental studies of Howard and co-workers (Marr et al. 1994, Benish et al. 1995), the collected tar material included the PAHs starting from about two aromatic rings and higher. Therefore, for the consistency with the experimental analysis, the mass growth rate of tar was evaluated using the computed rates of change for the PAHs starting from naphthalene. The computed masses of "tar" material and soot are presented in Figure 1a. It should be emphasized, however, that the present model of soot mass growth considers the contributions of the PAH compounds starting from pyrene, hence, the computed soot growth rate, in fact, did not have any contribution from 2-3 ring PAHs, and, equally, the calculated 2-3 ring PAH concentrations were unaffected by soot formation. Following the same approach as it was done in the reduction of the experimental data, the rates of "tar" and soot mass growth are obtained using the computed linear flame velocity (Figure 1b). Having all this information, it is possible now to evaluate the collision efficiencies defined by Eqs. (1.5) and (1.6). These results are presented in Figure 2a. As can be seen, the predicted values agree almost quantitatively with the data reported by Benish et al. Moreover, the contributions of tar and C_2H_2 calculated from Eq. (1.3) (Figure 2b) indicate the "dominant" role of tar material as soot growth species, in agreement with the conclusions made by Benish et al.

The presented numerical test demonstrates that the model of soot formation which suggests the leading role of C_2H_2 as soot growth species do not contradict the experimental results of Benish et al. It also illustrates the fact that the analysis conducted by Benish et al. cannot be served as a proof of the dominance of tar contribution in soot mass growth.

The mechanism of mass transfer from acetylene to soot, expressed by Eqs. (1.1) and (1.2) is shown schematically in Figure 3. It has two pathways: the "direct" route via reaction of C_2H_2 with soot (I), and "indirect" route which goes through tar growth (II-III). As can be seen in Figure 2b, the rate of tar growth is substantially lower than the rate of soot growth. As was discussed above, both acetylene and tar soot growth hypotheses can explain the observed trend. On one hand, the direct route (I) can be dominant, while both (II) and (III) would be slow to explain the observed low rate of tar production. On the other hand, if the direct route (I) is slow, the rates of (II) and (III) are fast, i.e., tar is formed and consumed rapidly resulting in low net tar production. Thus, the information available from the experiment appears to be insufficient to prove or disprove either point of view. The answer depends on the ratio of the "channels" (I) and (II) which has to be guessed or estimated. The conclusions of Benish et al. in essence follow from the assumption (5) which suggests similar reaction probabilities for C_2H_2-soot and C_2H_2-tar collisions. The analysis of the modeling results, on the other hand, indicates that the kinetics of tar growth is more complex than that described by Eq. (1.2) and cannot be treated as a simple C_2H_2-tar reaction. According to the model predictions, the ultimate tar mass comes from the reactions of smaller aromatic compounds with acetylene. These processes are strongly reversible which causes low net rate of tar production.

Jander, H. (1992) Privite communication.

Kazakov, A., Wang, H., and Frenklach, M. (1995) *Combust. Flame*, 100, 111.

Marr, J. A., Giovane, A., Longwell, J. P., Howard, J. B., and Lafleur, A. L. (1994) *Combust. Sci. Technol.* 101, 301.

Benish, T. G., Howard, J. B., and Lafleur, A. L. (1995) Paper 93 presented at the Fall Technical Meeting of the Eastern States Section of the Combustion Institute, Worcester, MA.

APPENDIX

THE DERIVATION OF MASS GROWTH RATES

1. Input Data.

T = 1650 K – the temperature;

$[C_2H_2] = 1.47$ Ã 10^{-7} mol/cm^3;

m_{tar} = 500 g/mol;

m_{C2H2} = 26 g/mol;

$[tar] = M_{tar}/m_{tar} = 2$ Ã $10^{-3}\ M_{tar}$ mol/cm^3;

d_{tar} = 10 Å;

d_{C2H2} = 3.4 Å;

®$_{soot}$ = 1.8 g/cm3;

$N_{soot} = 10^{11}$ cm^{-3}.

$$\bar{c}_{C_2H_2} = \sqrt{\frac{8RT}{\pi m_{C_2H_2}}} = 1.16 \times 10^5 \quad \text{cm/s;}$$

$$\bar{c}_{tar} = 2.64 \times 10^4 \text{ cm/s;}$$

$$d_{soot} = \left(\frac{6M_{soot}}{\pi \rho_{soot} N_{soot}}\right)^{1/3};$$

$$S_{soot} = \pi N_{soot} d_{soot}^2 = \pi N_{soot}^{1/3} \left(\frac{6}{\pi \rho_{soot}}\right)^{2/3} M_{soot}^{2/3} = 1.52 \times 10^4\ M_{soot}^{2/3}$$

2. Rates.

$$m_{C_2H_2} Z_{C_2H_2\text{-soot}} = \frac{m_{C_2H_2}}{4} S_{soot} \bar{c}_{C_2H_2} [C_2H_2] = 1.69 \times 10^3 M_{soot}^{2/3},$$

$$m_{tar} Z_{tar\text{-soot}} = \frac{m_{tar}}{4} S_{soot} \bar{c}_{tar} [tar] = 1.00 \times 10^8 M_{soot}^{2/3} M_{tar},$$

$$m_{C_2H_2} Z_{C_2H_2\text{-tar}} = \frac{\pi m_{C_2H_2}}{4} \left(d_{C_2H_2} + d_{tar}\right)^2 \bar{c}_{C_2H_2\text{-tar}} [C_2H_2][tar] = 7.8 \times 10^6 M_{tar}.$$

All rates are given in units g cm^{-3} s^{-1}, the units of M_{tar} and M_{soot} are g cm^{-3}.

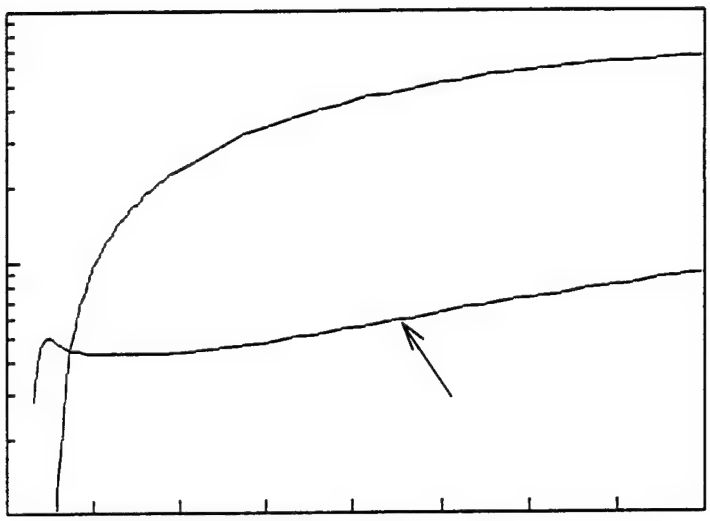

Figure 1a

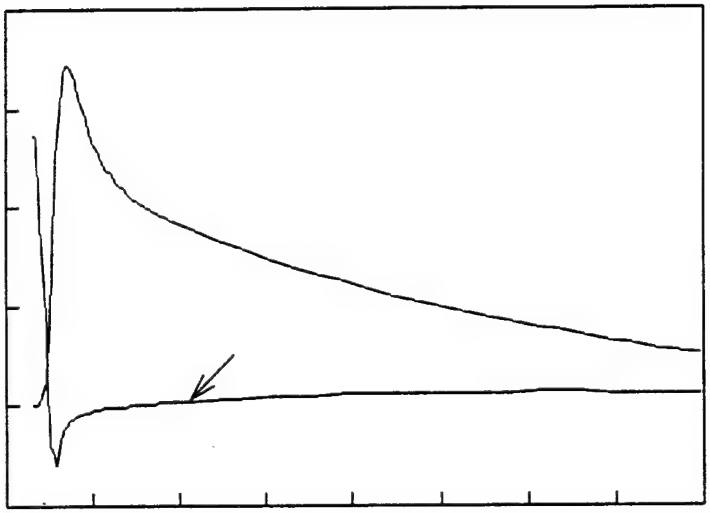

Figure 1b

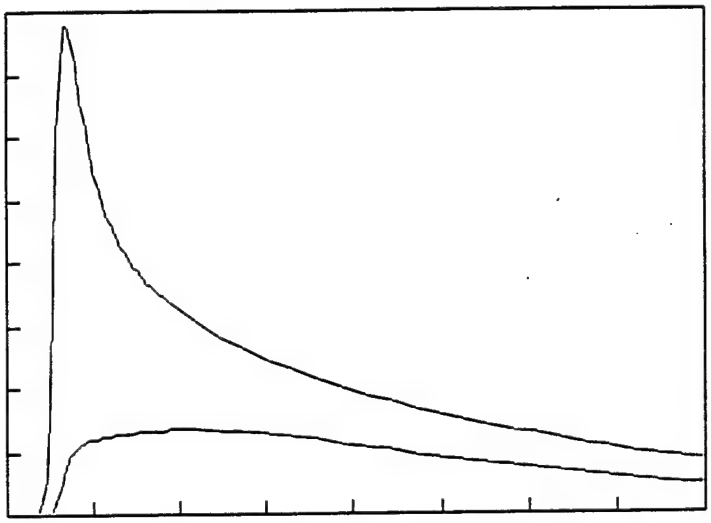

Figure 2b

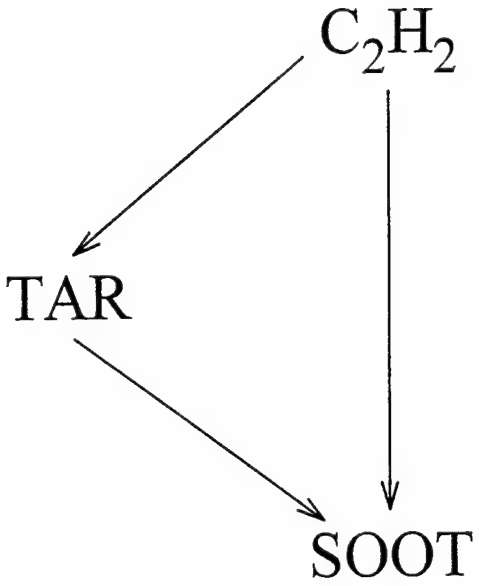

Figure 3

A Possible Pathway For PAH Production In Sooting Flames Involving Neutral Species.;

B. Weiner and M. Frenklach

Over the last few decades there has been much debate and analysis of the mechanism of soot formation in hydrocarbon fuel combustion.[1] It is agreed that there are various stages to this process, starting with gaseous precursor formation followed by particle nucleation, coagulation, agglomeration, and surface growth and oxidation. However, the details of the mechanism have not been definitively established due to the complexity of the process and the difficulty of the process and the difficulty in obtaining comprehensive and unambiguous experimental data. Both ionic and neutral species have been observed in sooting flames, however under normal flame conditions, the concentration of neutrals is seen to be much higher and would thus seem to favor a free radical mechanism.

The objective of the present study is to investigate theoretically a model chemical reaction, representative of reaction steps that may play a role in molecular growth of Poly Aromatic Hydrocarbons (PAH's) in hydrocarbon flames. The neutral C_3H_3• radical is found in high concentrations in sooting flames, thus a very plausible chain of reactions that can serve as a template for PAH growth in such an acetylenic rich atmosphere is

$$C_3H_3\bullet + C_2H_2 \rightarrow C_5H_5\bullet$$
$$C_5H_5\bullet + C_2H_2 \rightarrow C_7H_7\bullet$$

As the formation of multi ringed aromatics are anticipated to follow the same or a very similar mechanism to the formation of the first ring, an analysis of such an initial reaction chain will be a guide for PAH growth.

The calculations were carried out using the Gaussian 92 Quantum chemistry program. Molecular geometry's were determined by finding local minima of the energy with respect to variations of the nuclear framework of the molecules and molecular fragments. The energy was calculated within the Unrestricted Hartree Fock (UHF) approximation using a 6-31g** basis set. Transition states between various isomers were determined by finding saddle points of the UHF energy functional corresponding to one negative root of its Hessian matrix. At these stationary geometry's (local minima and saddle points) energy corrections were calculated using spin projected Moeller Plesset Second Order (PMP2) perturbation theory. All the calculations refer to energies at 0K. Various isomers of $C_3H_3\bullet$, $C_5H_5\bullet$, and $C_7H_7\bullet$ and rearrangement pathways between the radicals $C_5H_5\bullet$, and $C_7H_7\bullet$ were studied. The most energetically favorable pathway was selected that leads from $C_3H_3\bullet$ to an aromatic hydrocarbon in an acetylenic atmosphere. The initial stages of this pathway are displayed in figures 1 and 2. The first figure shows the energetics as calculated within the UHF approximation, while the second figure the energetics that include corrections calculated within spin projected perturbation theory, PMP2. The energies shown are with respect to the lowest energy isomer of $C_5H_5\bullet$ found from the Gaussian 92 calculations. The first relative energy shown on the far left of figures 1 and 2 is for well separated $C_3H_3\bullet$ and C_2H_2, to the right of this we display the isomer of $C_5H_5\bullet$ and its relative energy that is formed from the initial addition reaction. This reaction has no electronic barrier nor does the next one, that involves a bond formation and transport of the radical site,

producing the species shown third from the right. This species then undergoes a hydrogen rearrangement with a barrier of approximately 29.95 kcals, as calculated with both the UHF and PMP2 methods, to form the radical shown on the far right hand side of figures 1 and 2. The last stage in this reaction sequence is the only one with a barrier, as the forward activation energy required for this last step is much less than that released by the initial steps of this reaction sequence there is sufficient energy available for this reaction to occur. The backward activation energy barrier can be seen to be larger than the forward one, thus one expects these sequence of reactions to lead to the production of the isomer of $C_5H_5\bullet$ on the far right of this figure.

Starting from this isomer, again in an acetylenic atmosphere we display in figures 3 and 4 a sequence of reactions leading to an aromatic radical. This time the energies calculated within the PMP2 approximation are somewhat different from those calculated within the UHF one. The barriers calculated within the UHF ansatz are 20.2, 24.3, 20 and 23.6 kcal/mol above the energies of the starting reactants $C_5H_5\bullet$ and $C_3H_3\bullet$. The energy of 20 kcal/mol shown for the barrier between species 3 and 4 is estimated, as a fully converged transition state has not been obtained in this case, but a partially converged energy of ~20 kcal/mol has been obtained. The barriers calculated with the PMP2 correction are 7.9, 13.3, 15 and 7.9 kcal/mol above the energies of the starting reactants. The barrier between species 3 and 4 is again estimated this time as 15 kcal/mol in line with the general decrease of the PMP2 barriers compared to the UHF ones. Note that for the transition states 2 -3, 3-4, 4-5 and 5-6 the actual activation energies are larger as the energies of these stable intermediates are below that of the starting species as shown. The largest barrier in the PMP2 case (which is the more reliable as it is a more accurate approximation) is ~38 kcal/mol, though this might be an overestimate as it depends on 15 kcal/mol

guessed as an upper limit for the transition state 3-4. From an energy point of view the reaction sequence should proceed from the left hand side species shown in figure 2 to the aromatic radical shown on the right hand side of figures 4, as approximately 81 kcals/mol of energy is released in the first sequence shown (figures 2) and the backward activation energies are greater than the forward ones in both sequences (figures 2 and 4). A more detailed kinetic study based on these results needs, however, to be carried out in order to see if such a conclusion is indeed supported. The reaction sequence of figures 3 and 4 display a rather novel rearrangement from a five membered (structures 2 and 3) to a six membered ring (structure 5) via a tricyclic intermediate (structure 4). The bond that breaks during the transition state 4-5 is marked on the figures with a wavy strike-through symbol.

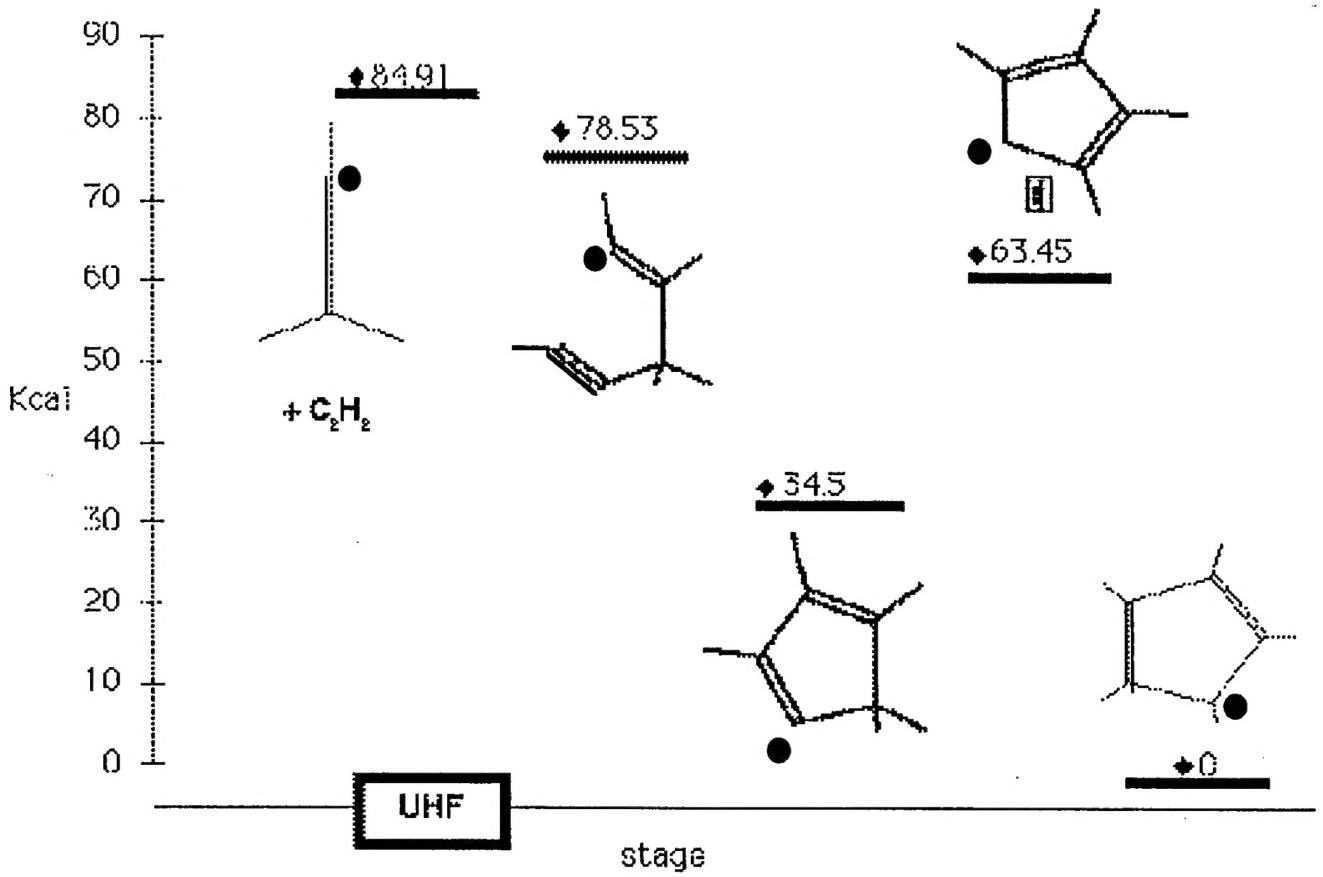

Figure 1: Reactions starting from C_3H_3 radical plus C_2H_2 followed by rearrangements calculated using the UHF approximation. The energies are in kcal/mol relative to the energy of the final product at the right hand side.

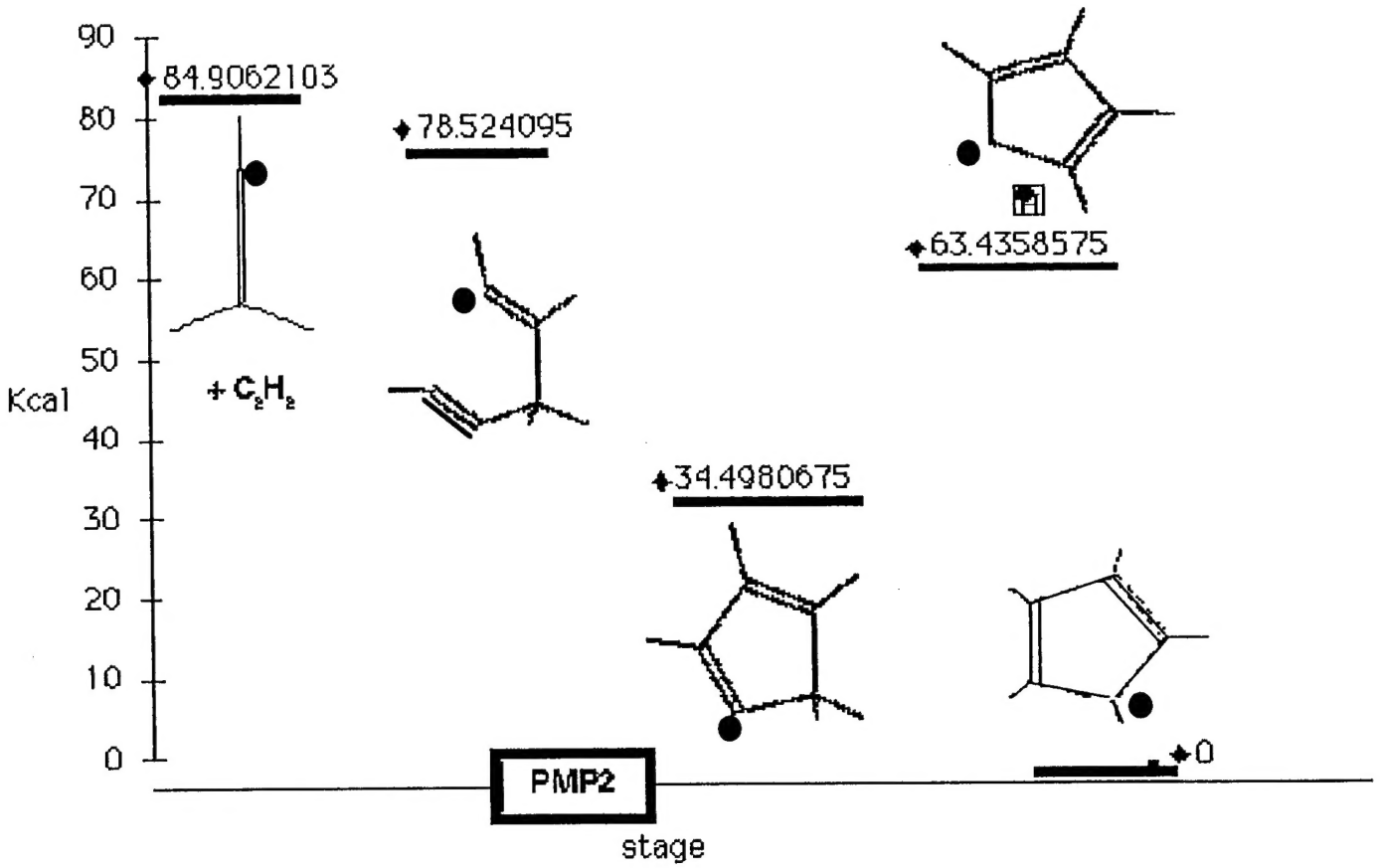

Figure 2: Reactions starting from C_3H_3 radical plus C_2H_2 followed by rearrangements calculated using the spin projected MP2 approximation. The energies are in kcal/mol relative to the energy of the final product at the right hand side.

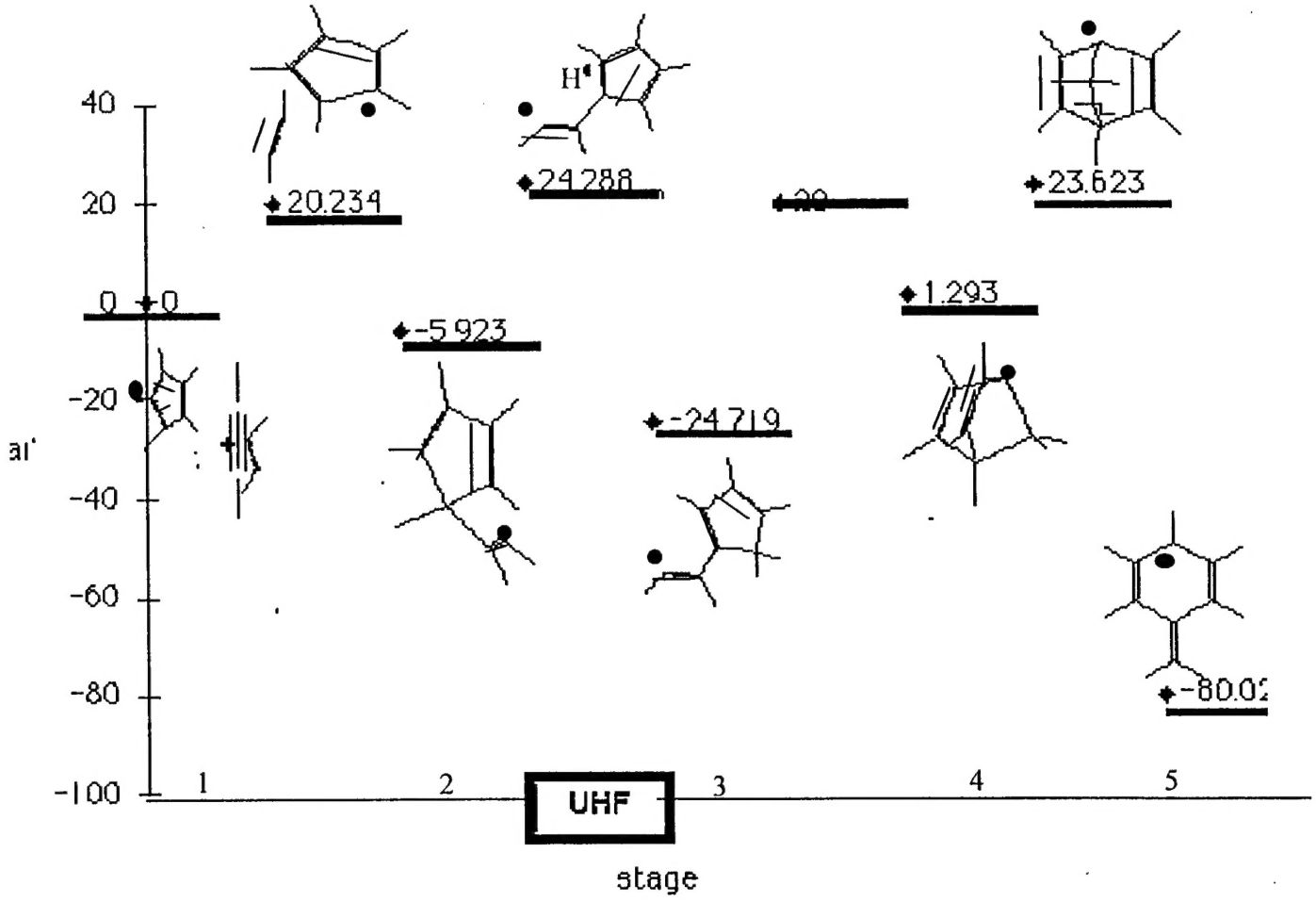

Figure 3: Reactions starting from C_5H_5 radical plus C_2H_2 followed by rearrangements calculated using the UHF approximation. The energies are in kcal/mol relative to the energy of reactants at stage 1.

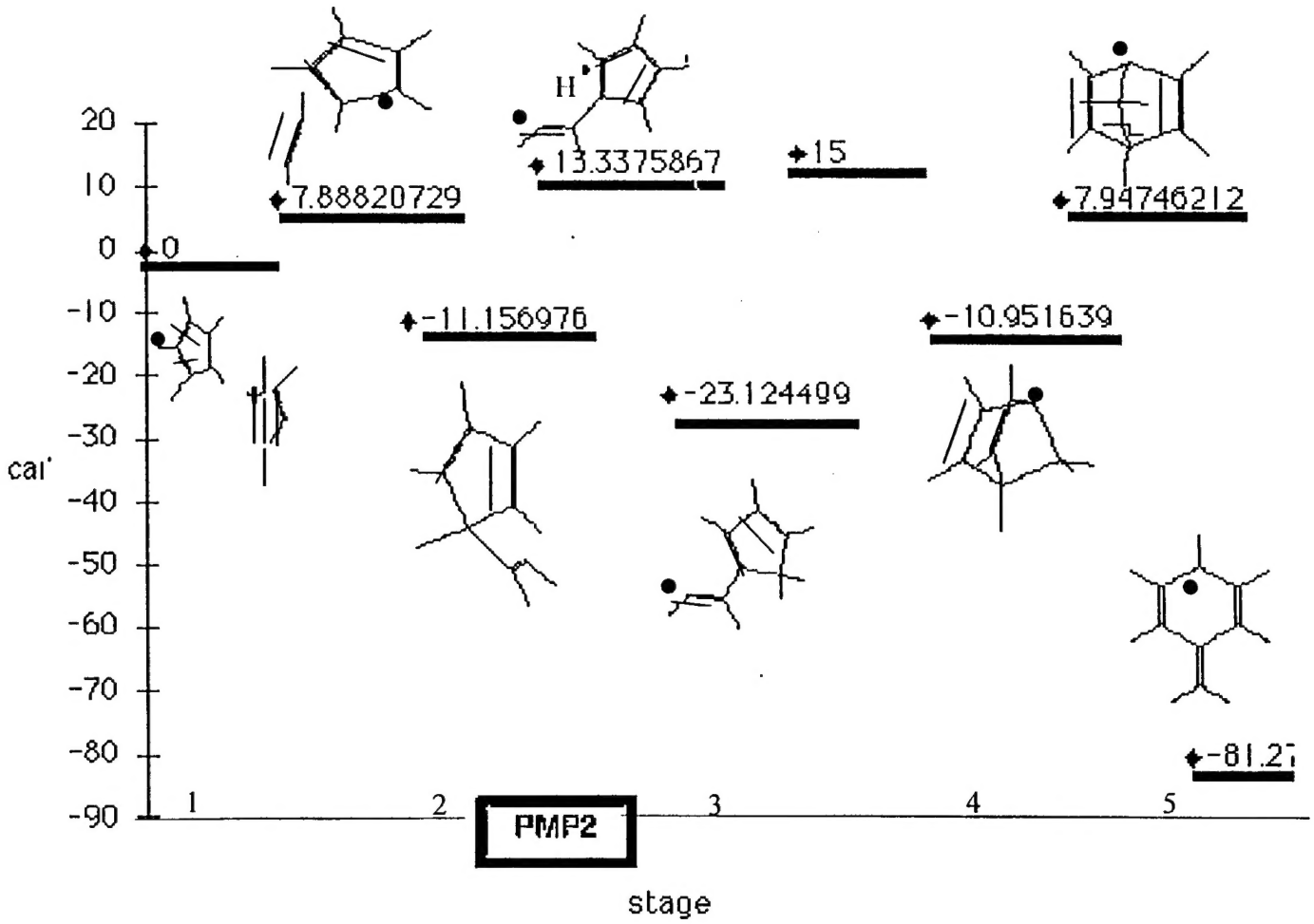

Figure 4: Reactions starting from C_5H_5 radical plus C_2H_2 followed by rearrangements calculated using the spin projected MP2 approximation. The energies are in kcal/mol relative to the energy of reactants at stage 1.